CrossMark

RESEARCH PAPER

Performance of the Prestressed Composite Lining of a Tunnel: Case Study of the Yellow River Crossing Tunnel

Fan Yang[1] · Shengrong Cao[1] · Gan Qin[1]

Abstract This paper presents the performance of a new prestressed composite lining applied in shield tunnels for water conveyance. The Yellow River Crossing Tunnel of the Middle Route Project of the South-to-North Water Division Project is adopted in this study as a case, and a three-dimensional finite element model is established to analyse the stress distribution and deformation feature of the prestressed composite lining when the tunnel is under the assembly condition, the tension condition and the water-filled condition. The finite element model is verified by comparing with the results of the full-scaled simulation experiment. The calculation and analysis results reveal that further open of the segmental joint gaps can be limited and full circumferential compression of the secondary lining can be realized when the tunnel is under the water-filled condition, which are conducive to long-term operation of the prestressed composite lining. The membrane has a significant effect on preventing stresses from being transmitted between the segmental lining and the secondary lining. The numerical calculations are verified by the results of the full-scaled simulation experiment, and the three-dimensional numerical model combined with the analysis method used can simulate the structural characteristics and the bearing mechanism of the prestressed composite lining.

1 Introduction

The prestressed composite lining is a kind of tunnel structure composed of an outer segmental lining and an inner secondary prestressed lining with circular anchor cables. This secondary prestressed lining can overcome the shortcoming of the small tensile strength of the concrete so that the concrete material can be fully utilized to withstand internal high pressures [1, 2]. Therefore, compared with ordinary double linings, the prestressed composite lining is more suitable for the shield tunnels with high internal pressure. This new structure of the prestressed composite lining has attracted a lot of attention for the first application to the South-to-North Water Diversion Project in China.

Shield tunnels with monolayer segmental lining have appeared worldwide with the spread of the tunnel boring machine technology. The numerical models of the monolayer segmental lining mainly include the uniform ring model, multi-hinge ring model, beam-spring model, and shell-spring model [3–6]. Moreover, three-dimensional finite element models have been suggested to consider the three-dimensional effects of the segments [7]. With the wide use of segmental lining for subway shield tunnels and highway shield tunnels, scholars have conducted extensive research on the above calculation models and obtained many valuable research results that can provide references for calculating the segmental lining of prestressed composite lining.

✉ Shengrong Cao
  shrcao@whu.edu.cn

  Fan Yang
  fyang@whu.edu.cn

  Gan Qin
  gqin@whu.edu.cn

[1] State Key Laboratory of Water Resource and Hydropower Engineering Science, No. 299 BaYi Road, Wuhan 430072, People's Republic of China

Springer

In recent years, the monolayer circular prestressed concrete lining has been applied in some large pressure tunnels in China, such as the water conveyance tunnel of Geheyan Hydropower Station, the water conveyance tunnel of Tianshengqiao First Cascade Hydropower Station, and the desilting tunnel of Xiaolangdi Project. The prestressed anchor cables are usually equivalent to a thin steel plate, and the prestresses are simplified as a uniform radial pressure in the design for the prestressed lining with circular anchor cables [8, 9]. This simplified method is not suitable to be used as the only basis of the design for the prestressed lining with circular anchor cables. Additionally, the results should be verified by three-dimensional finite element analysis or physical model experiments.

The prestressed composite lining is a combination of the segmental lining and the prestressed lining with circular anchor cables. This application is the first time that prestressed composite lining has been applied to tunnel projects. Therefore, the related engineering experience is limited, and there are few calculation models that can be directly referenced. Some researches on the composite lining mainly focus on the ordinary double lining for shield tunnel. And the existing numerical models of the composite lining are mostly based on the Guidelines for Design of Shield Tunnel Lining issued by the International Tunnelling Association (ITA). In the case of a double shell structure, the methods for computing the member forces of the secondary lining can be divided into the bedded frame model method and the elastic equation method [10]. Based on the bedded frame model method, some improved numerical models are proposed [11–14]. As shown in Fig. 1, there are four main numerical models. In Model I, a radial beam is used to simulate the transmission of the stress on the contact surface between the segmental lining and the secondary lining. However, this model leads to an abrupt change in the bending moment at the fixing point of the segmental lining or secondary lining. In Model II, a radial spring and a tangential spring are used to simulate the transmission of the radial stress and the tangential stress on the contact surface, respectively. These two models cannot avoid the appearance of radial tension on the contact surface. In Model III, a radial compression bar is suggested to replace the radial spring. When the compression bar element is in tension, its axial force becomes zero. In Model IV, contact elements are employed to simulate the stress transmission on the contact surface, and a friction coefficient is needed to reflect the transmission of the tangential stress.

Model I–Model IV have been used to calculate the composite lining with an ordinary concrete lining as the secondary lining. However, in the case of the Yellow River Crossing Tunnel, the secondary lining is a prestressed lining with bonded circular anchor cables. The distribution of the prestresses along the prestressed anchor cable length direction is not uniform, and the layout of the anchor cables along the axial direction must be considered. Therefore, the stress distribution of the secondary lining is more complex than that of the ordinary concrete lining and must be simulated using a three-dimensional solid model. However, the four models above are all based on the two-dimensional beam-spring model or the three-dimensional shell-spring model, and the calculation methods of the stiffnesses of the springs or the bars are not suitable for the three-dimensional solid model. In addition, the segmental lining and the secondary lining are bonded together only at the bottom, while the others are separated by the membrane which is an important structure that is not considered in the above Model I–Model IV. Therefore, the actual stresses of the segmental lining and the secondary lining cannot be calculated well if the above numerical models are used directly.

As the prestressed composite lining is applied for the first time in tunnel projects, the related documented experimental, numerical and analytical results exist in literature concerning the functioning of the prestressed composite lining are limited. The performance of this new tunnel lining is still not clarified. Based on the above studies, a three-dimensional solid model is established by the finite element method to analyse the prestressed composite lining of the Yellow River Crossing Tunnel. Solid elements are used to simulate the soil, the segmental lining and the secondary lining. Spring elements are used to simulate the membrane. The interaction between the segments is considered. The performance of each component of the prestressed composite lining and the interaction between the segmental lining and the secondary lining are calculated and analysed when the tunnel is under the assembly condition, the tension condition and the water-filled condition. The numerical calculation is verified by the full-scaled simulation experiment. According to the analyses of the numerical calculation and the experimental results, the structural characteristics of the prestressed composite lining of the Yellow River Crossing Tunnel are introduced in detail in this paper.

2 Case Studied Tunnel

The South-to-North Water Diversion Project (SNWD) is the most expensive and extensive project ever undertaken in China. This project consists of the Eastern Route Project (ERP), the Middle Route Project (MRP) and the Western Route Project (WRP). Several generations of technical personnel from China and all over the world have carried out survey, planning, design and research work for the MRP since the 1950s. The MRP has been in use since December 12, 2014.

The Yellow River Crossing Project is a key project of the MRP-SNWD. The Yellow River Crossing Tunnel is the largest building with the longest construction period, the most advanced technology and the most difficult construction in the SNWD. The Yellow River Crossing Project is widely known as the most ambitious water conservancy project that crosses great rivers in the history of mankind. The two parallel tunnels are the most impressive and important buildings in the entire Yellow River Crossing Project. The total length of each tunnel is 4250 m and the length of the Yellow River Crossing Tunnel is 3450 m. The excavation diameter of each tunnel is 8.7 m, and the design flow rate is 265 m³/s. The longitudinal profile of the Yellow River Crossing Project is shown in Fig. 2. The Yellow River Crossing Tunnel has the characteristics of large scale, deep buried depth, large flow rate, high internal water pressure, and poor geological conditions. These

characteristics are not conducive to the construction and operation of the tunnel. It is very important to prevent high-pressure water from leaking out and to avoid seepage failure of the soil around the tunnel.

The Yellow River Crossing Tunnel passes through soft soil and is constructed by the shield tunnelling method. The tunnel needs to be quickly supported by assembled precast segments to withstand the soil pressure and the external water pressure during excavation to avoid large deformations of the excavation face and to speed up the construction progress. The internal water pressure in the centre of the tunnel is more than 0.5 MPa when the tunnel is under the water-filled condition. If the internal water pressure is borne only by the segmental lining, the segmental joints will be large opening, resulting in water seepage. Therefore, a secondary lining is needed to improve the bearing capacity of the tunnel lining and to simultaneously improve

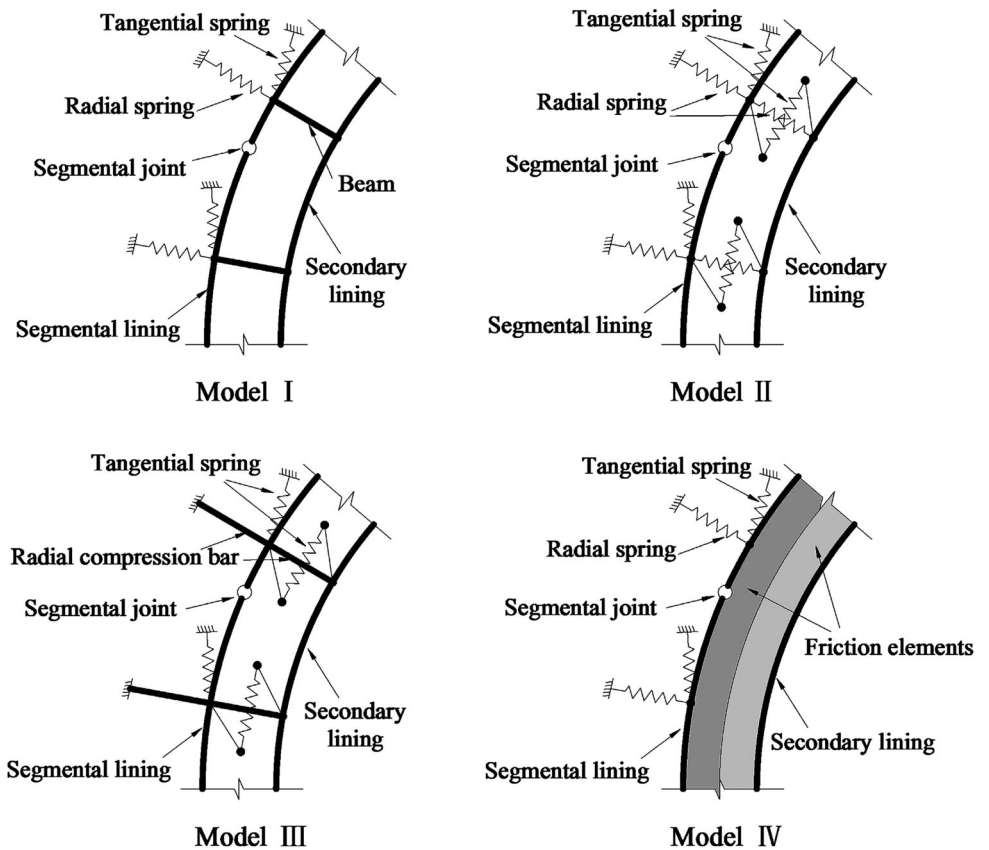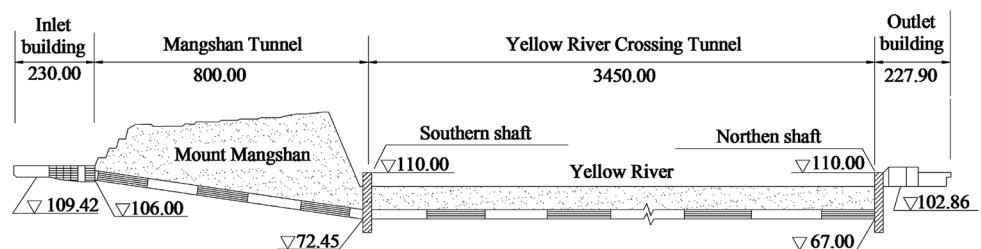Fig. 1 Numerical models of the composite lining

Fig. 2 Longitudinal profile of the Yellow River Crossing Project (unit: m)

the tunnel inner surface smoothing. As the post-prestressed concrete lining with circular anchor cables has advantages with respect to structure strengthening, high material utilization and water proof strengthening, it is proposed as the secondary lining. The bottom of the secondary lining concrete is directly poured on the segmental lining, and the others are separated from the segmental lining by the membrane which is shown as a red line in Fig. 3. The external load of the tunnel is expected to mainly be borne by the segmental lining, and the internal water pressure is expected to mainly be borne by the secondary lining. In addition, the membrane can play a role in waterproof and drainage.

3 Full-Scaled Simulation Experiment and Materials

3.1 Model Dimensions

An underground full-scaled simulation experiment is carried out. The model is embedded underground with embedded depth and soil water condition similar to the real project, and water pressure is carried out by elevating the water tank to the design height [15].

The experimental model dimensions are showed in Figs. 3 and 4. The model has an axial length of 9.6 m. Segment external diameter is 8.7 m; internal diameter is 7.9 m; width is 1.6 m. The segmental lining is erected

by staggered format (Fig. 5). The segments are connected by M32 straight bolts. Pre-tightening force of each bolt is 100 kN. The membrane composes of three layers of materials; the middle layer is impermeable, and the others are elastic permeable. The membrane has a total thickness of 6×10^{-3} m and annularly encloses a circumferential angle of 301.548°. The secondary lining external diameter is 7.9 m; internal diameter is 7.0 m. The bottoms of both the secondary lining and the segmental lining are bonded together at a circumferential angle of 58.452°. The secondary lining concrete is poured when the segmental lining has already borne the external pressure and achieved stability. The prestressed anchor cables tensioning begins when the secondary lining concrete pour is completed and the concrete strength can meet the requirements. As shown in Fig. 4, the preformed grooves are in the lower half of the secondary lining and the centre lines of the grooves are located at the angles of 96°, 134°, 226° and 264°. The distance between adjacent grooves is 0.45 m along the axial direction. Small relaxation steel wire strands of 12φj15.24, which have a design tension stress of 1395 MPa, are used as prestressed anchor cables.

Stresses of the Section I, Section II and Section III are observed in the full-scaled simulation experiment (Fig. 4). As shown in Fig. 3, the numbers in the parentheses are the dimensions of the observation sections. Figure 3 also shows the distribution of the observation points. A column coordinate system is used in Figs. 3, 4 and 5.

Fig. 3 Cross section of the prestressed composite lining (unit: m)
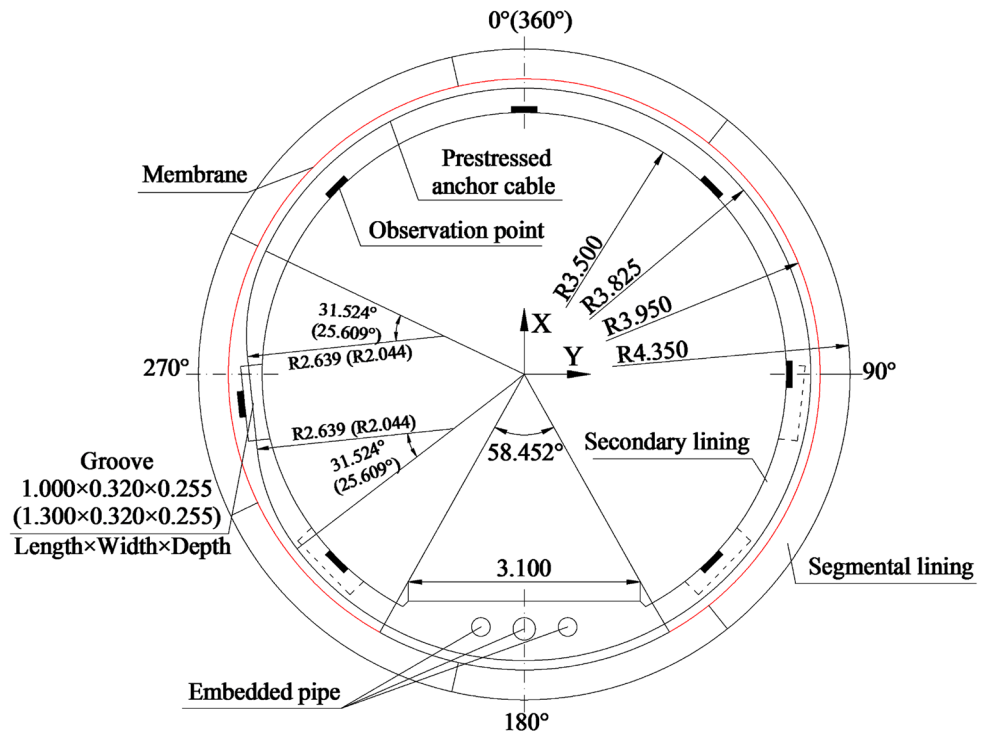
Fig. 4 Grooves layout along the axial direction (unit: m)
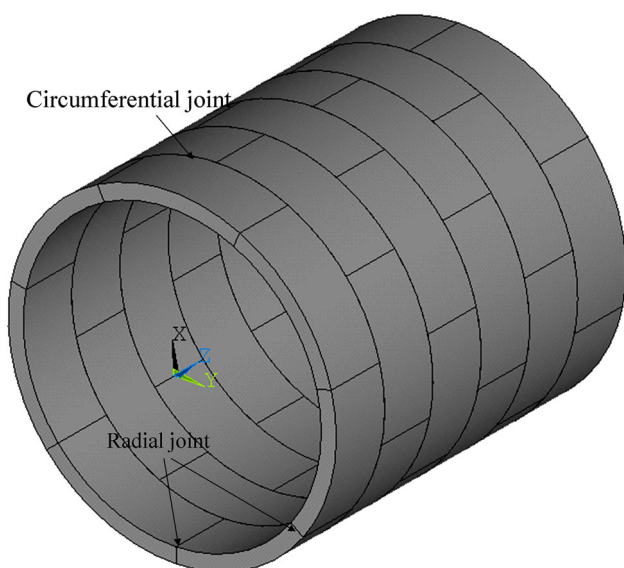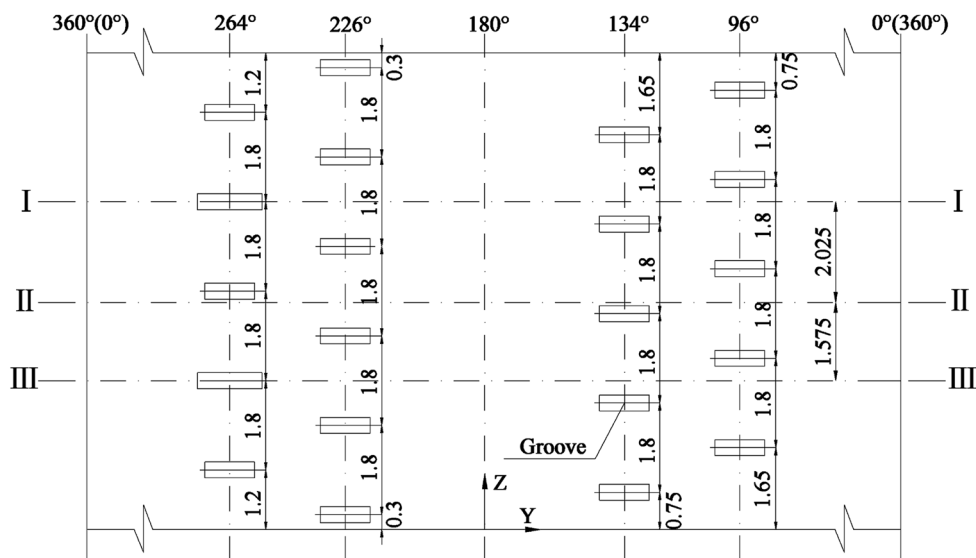
Fig. 5 Joints between segments

Fig. 6 Material properties for soil

Note: γ' = effective unit weight; φ = friction angle; c = cohesion; E = elastic modulus of soil, 40 Mpa; μ = Poisson's ratio, 0.3.

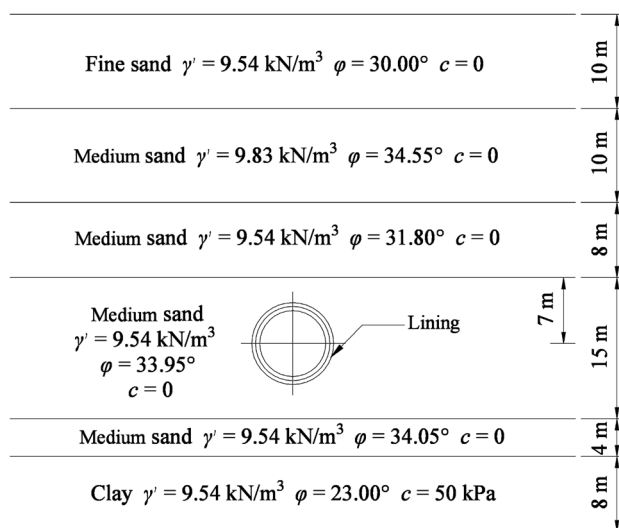## 3.2 Model Materials

The soil above the Yellow River Crossing Tunnel is the medium granular sand, and the clay is under the tunnel. Figure 6 presents the material properties for the soil. The material properties for the lining are listed in Table 1.

4 Numerical Simulations

4.1 Numerical Models

Finite element method is an efficient and mature calculation method, which has been widely used in engineering research [16]. A three-dimensional solid model is established for the prestressed composite lining of the Yellow River Crossing Tunnel. The dimensions of the model are shown in Fig. 7. The elastic–plastic constitutive model based on Drucker–Prager yield criterion is used for the soil. The stress–strain relationship of the segmental lining, the secondary lining, the membrane and the prestressed anchor cables are idealized to be linear-elastic.

Eight-node three-dimensional solid elements are used for the soil and concrete. Two-node link elements are used for the prestressed anchor cables. The finite element model of the secondary lining is shown in Fig. 8. Two-node beam elements are used for the radial bolts and circumferential bolts (Fig. 9). The contact surface between the segmental lining and the soil and the contact surface between the
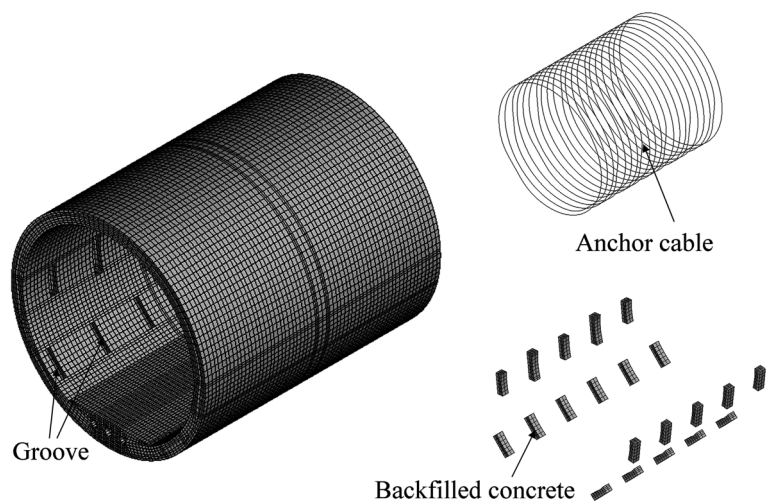
Table 1 Material properties for lining

Type	Material	Young's modulus (kN/m^2)	Poisson's ratio	Unit weight (kN/m^3)
Segmental lining	C50 concrete	3.45×10^7	0.167	25.5
Secondary lining	C40 concrete	3.25×10^7	0.167	24.5
M32 bolt	Steel	2.1×10^8	0.3	78.5
Anchor cable	Steel	1.95×10^8	0.3	78.5
Membrane	–	1.5×10^3	0.3	–
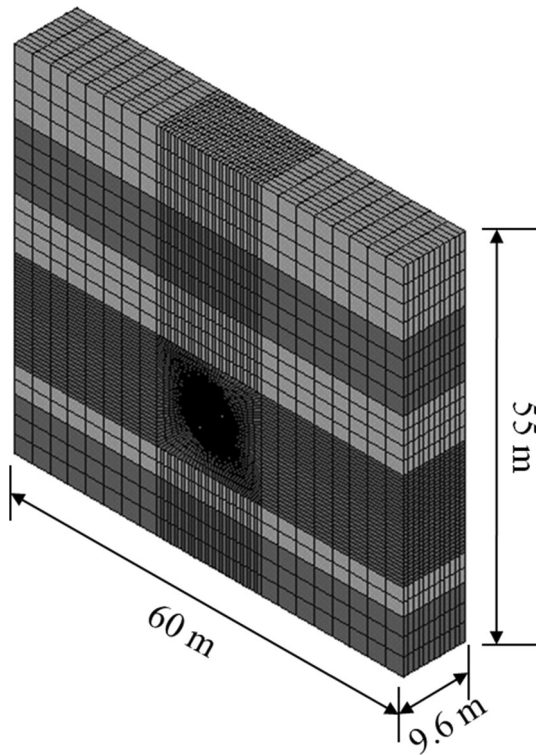
Fig. 7 Dimensions of the finite element model

adjacent segments are simulated by contact elements (Figs. 9, 10). These "face-to-face" elements can simulate cold interface conditions transmitting only compression in the direction normal to the surfaces and shear in the tangential direction [17, 18]. A friction coefficient of 0.3 is used to simulate the tangential behavior and the Lagrange and penalty method is used as the contact algorithm [19]. The incremental scheme follows the Newton–Raphson method [20].

The bottom of the segmental lining and the secondary lining are considered to be bonded completely and the relative slip is prohibited, while the others are separated by the membrane. As shown in Fig. 10, the membrane is simulated by three springs: one normal spring and two shear springs. The radial spring behaves as a compression support and does not contribute to tension. The stiffnesses of the springs are calculated as follows:

$$k_r = \frac{E \times A}{t} \tag{1}$$

$$k_\tau = \frac{G \times A}{t} \tag{2}$$

where k_r is the compression stiffness of a single radial compression spring; k_τ is the compression stiffness of a single tangential compression spring; E is the Young's modulus of the membrane; G is the shear modulus of the membrane; A is the corresponding area of a single spring; and t is the thickness of the membrane.

In the model, the nodes in the bottom surface are restrained against all displacements in three directions, and the nodes around the model are restrained against the
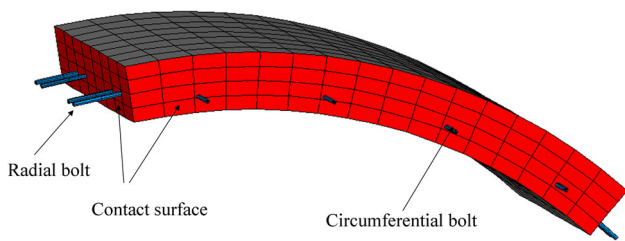
Fig. 8 Finite element model of the secondary lining

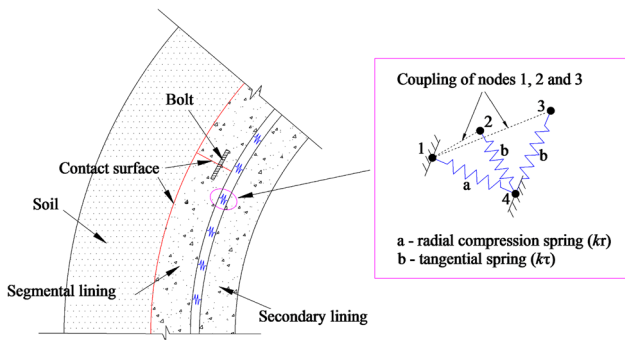**Fig. 9** Bolts and contact surfaces between segments

Fig. 10 Interaction between segmental lining and secondary lining

displacement in the vertical direction except for the nodes in the top surface. The whole numerical model contains 170,498 elements and 173,885 nodes.

4.2 Load Combinations of Calculation Stages

According to the construction process and the operating conditions of the Yellow River Crossing Tunnel, the model is calculated in three stages. The first stage is under the assembly condition when the segmental lining is assembled and reaches stability. The second stage is under the tension condition when the secondary lining concrete is poured and the prestressed anchor cables are tensioned. The third stage is under the water-filled condition when the grooves are backfilled with concrete and the internal water pressure is applied. The load combinations of each working condition are shown in Table 2.

The external water pressure in the horizontal line of the tunnel centre is 0.323 MPa. The internal water pressure in the tunnel centre is 0.51 MPa when the tunnel is under the water-filled condition. Separate calculations of water and earth pressures can be used when the tunnel is covered by sandy soil [21]. The external water pressure is directly on the segmental lining and the effective unit weight of the soil is used.

Prestress loss of the anchor cables is inevitable because of the deformation of anchorages and the shrinkage of steel strands, the friction between the steel strand and the duct, the relaxation of the steel strand stresses and the shrinkage and creep of the concrete [22]. Therefore, the effective

prestresses of the anchor cables are equal to the design tension stresses minus all of the prestress loss. The effective prestresses along the circumferential angle are shown in Fig. 11. The prestresses are converted to initial temperature loads and applied to the anchor cable elements in the model [23]. The temperature loads can be calculated by

$$T = -\frac{\sigma_{pe}}{E\alpha} \tag{3}$$

where T is the temperature load applied to the anchor cable elements; σ_{pe} is the effective prestress of the anchor cables; E is the elastic modulus of the anchor cables; and α is the linear expansion coefficient of the anchor cables.
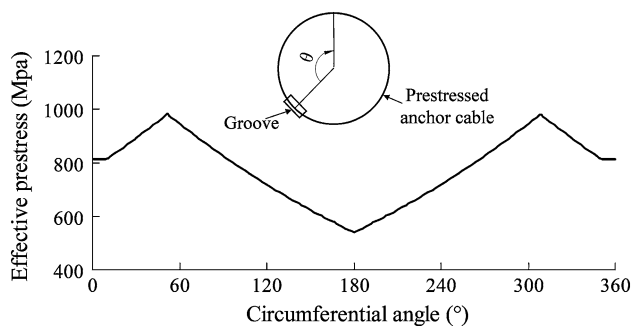
5 Results and Discussion

5.1 Circumferential Stresses of the Segmental Lining

The soil pressure and the external water pressure are both borne by the segmental lining under the assembly condition. The circumferential stresses of the segmental lining are presented in Fig. 12. Because the deformation shape of the tunnel is a squashed oval, circumferential tensions occur on the extrados surface of the springline, the intrados surface of the crown and the intrados surface the bottom. Meanwhile, the radial joints of the segments are opening there. The maximum joint gap is about 0.08 mm and the maximum depth of the joint gaps is about a quarter of the segment thickness.
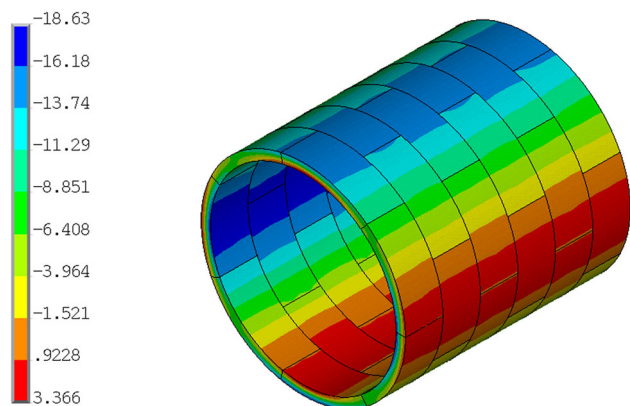
The circumferential stress distribution of the segmental lining except the bottom under the tension condition and the water-filled condition are consistent with that is under the assembly condition. To further mutual contrast, the circumferential stresses of the nodes which are in the middle ring of the segmental lining section (Z = 5600) are analysed under the three conditions (Fig. 13). The representation of the circumferential stresses is presented in a polar system of coordinates in Fig. 13. According to the calculation results, the circumferential stresses of the upper part of the segmental lining under the three conditions are similar. It may be because the upper parts of the segmental lining and the secondary lining are separated by the membrane, which can prevent stresses from being transmitted from the secondary lining to the segmental lining. The circumferential compression stresses of the bottom under the tension condition are larger than those under the assembly condition, because the secondary lining and the segmental lining are bonded together at the bottom and the prestresses of the secondary lining can be transmitted to the bottom of the segmental lining. The circumferential compression stresses of the bottom under the water-filled

Table 2 Load combinations of working conditions

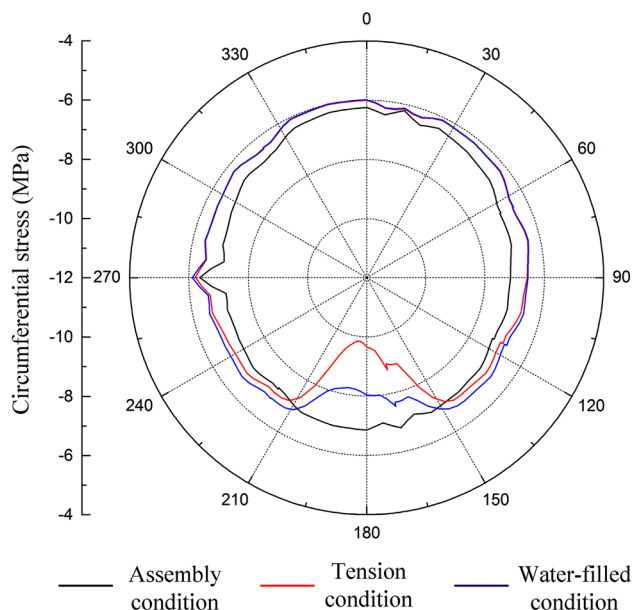| Working condition	Gravity	Soil pressure	Bolt pre-tightening force	External water pressure	Anchor cable prestress	Internal water pressure
Assembly condition	√	√	√	√		
Tension condition	√	√	√	√	√	
Water-filled condition	√	√	√	√	√	√

Fig. 11 Effective prestresses along the circumferential angle

Fig. 12 Circumferential stresses of the segmental lining under the assembly condition (unit: MPa)
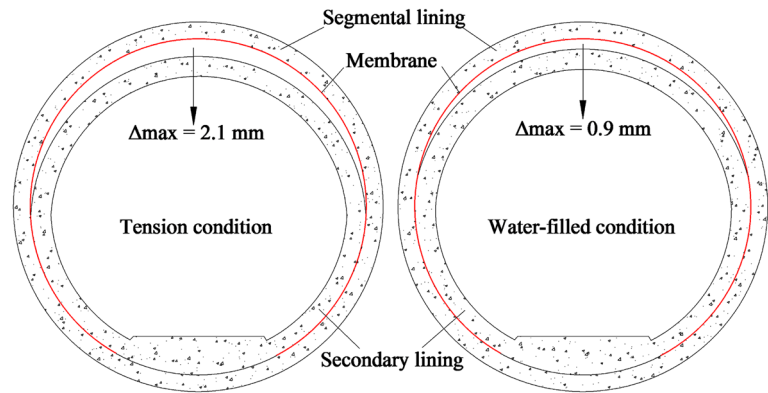

Fig. 13 Circumferential stresses of the nodes in the middle ring of the segmental lining

5.2 Interface Gap Between the Segmental Lining and the Secondary Lining

The bottoms of both the secondary lining and the segmental lining are bonded together at a circumferential angle of 58.452°, and the others are separated by the membrane. The lining deformations are shown in Fig. 14. The secondary lining shrinks inward under the tension condition because of the prestress. The gap (Δ) above the springline of the lining is open and the maximum gap that occurs at the top position is about 2.1 mm. Therefore, stresses can not be transmitted from the upper part of the secondary lining to the segmental lining. The radial compression springs below the springline of the lining are compressed. It means that the membrane is compressed there. According to the forces of the springs, the compression stresses of the membrane are very small and the maximum compression stress is about −0.08 MPa (negative values represent compressive stresses).

condition are smaller than those under the tension condition, because the internal water pressure can also be transmitted to the bottom of the segmental lining.

Only the joint gaps on the extrados surface of the tunnel springline are increased because of the internal water pressure. However, by comparing the water-filled condition with the assembly condition, the maximum increment of the gap is almost not more than 0.01 mm, and the increases of the circumferential stresses caused by the internal water pressure are not obvious at most positions of the segmental lining (Fig. 13). Therefore, it can effectively limit the segmental joints to being further open and reduce the infiltration of external groundwater to improve the stability of the segmental lining.

Fig. 14 Lining deformations (enlarge 200 times)

The secondary lining expands outward under the water-filled condition because of the internal water pressure. Therefore, the gap is smaller than that is under the tension condition and the maximum gap that occurs at the top position is about 0.9 mm. Both the number and the average forces of the compressed radial springs under the water-filled condition are slightly larger than those under the tension condition. However, according to the forces of the springs, the maximum compression stress of the membrane is less than −0.09 MPa. So the stresses transmitted from the secondary lining to the segmental lining through the membrane are very small when the prestresses or the internal water pressures are applied on the secondary lining.

5.3 Circumferential Stresses of the Secondary Lining

As indicated by the analysis above, the prestresses and the internal water pressures are mainly borne by the secondary lining because of the membrane. The stress distributions of the secondary lining under the tension condition and the water-filled condition are complex. Because the distribution of the effective prestresses along the prestressed anchor cable length direction are not uniform and the curvature radii of the prestressed anchor cables near the grooves are changed, and the grooves have a weakening effect on the secondary lining concrete. Section I and Section II are chosen as the typical sections to analyse the circumferential stress distribution (Fig. 4).

The circumferential stress distributions of Section I and Section II under the tension condition are shown in Fig. 15. As shown in Fig. 15, full circular compression is realized for both Section I and Section II. The circumferential stresses above the springline of the secondary lining are relatively uniform. The maximum circumferential compression stress occurs on the intrados surface of the springline. Comparing the circumferential stresses of the bottom with the circumferential stresses of the other parts, it can be seen that the circumferential compression stresses of the bottom are relatively small. It is because that the

secondary lining and the segmental lining are bonded together at the bottom of them, and the prestresses of the secondary lining bottom can be transmitted to the segmental lining. Moreover, the thickness of the secondary lining bottom is increased by applying a platform there. Comparing the Fig. 15b with the Fig. 15a, both the values and the distribution of the circumferential stresses are similar. Section II does not pass through the grooves; therefore, the circumferential compression stresses on the intrados surface of the left springline are relatively large, which is different from Section I.

The grooves are backfilled with concrete when the tunnel is under the water-filled condition. The circumferential stress distributions of Section I and Section II under the water-filled condition are shown in Fig. 16. Comparing the Fig. 16 with the Fig. 15, the circumferential compression stresses of both Section I and Section II under the water-filled condition are smaller than those under the tension condition because the internal water pressure is mainly borne by the secondary lining. However, full circular compression can also be realized for Section I and Section II except the backfilled concrete which is not influenced by the prestresses. The maximum circumferential tensile stress of the backfilled concrete is more than 4 MPa.

In practical projects, the grooves are filled with micro-expansive concrete so that all of the secondary lining concrete can be compressed, and the circumferential stresses of the upper semi-circle of the secondary lining are relatively uniform when the tunnel is under both the tension condition and water-filled condition, which are beneficial for the secondary lining working permanently and stably.

### 5.4 Comparison Between the Numerical Results and the Experimental Results

5.4.1 Results of the Full-Scaled Simulation Experiment

The circumferential stress increments of the secondary lining caused by the prestresses and the internal water pressures are observed in the full-scaled simulation

Fig. 15 Circumferential stresses of the typical sections under the tension condition (unit: MPa)

(a) Section I

(b) Section II
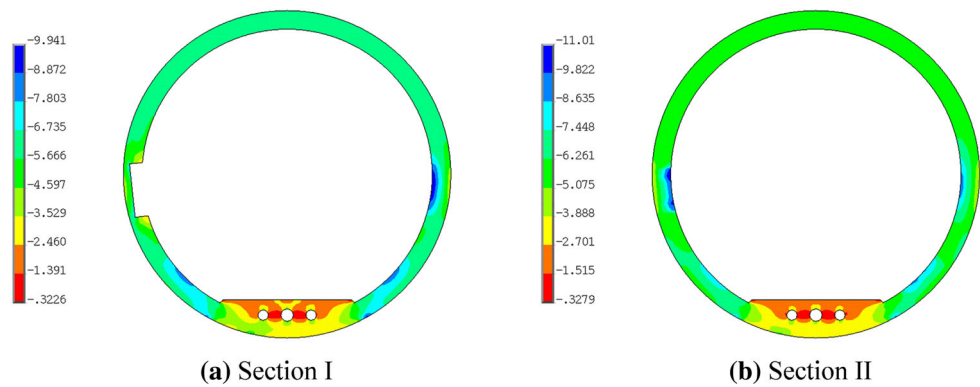
Fig. 16 Circumferential stresses of typical sections under the water-filled condition (unit: MPa)

(a) Section I
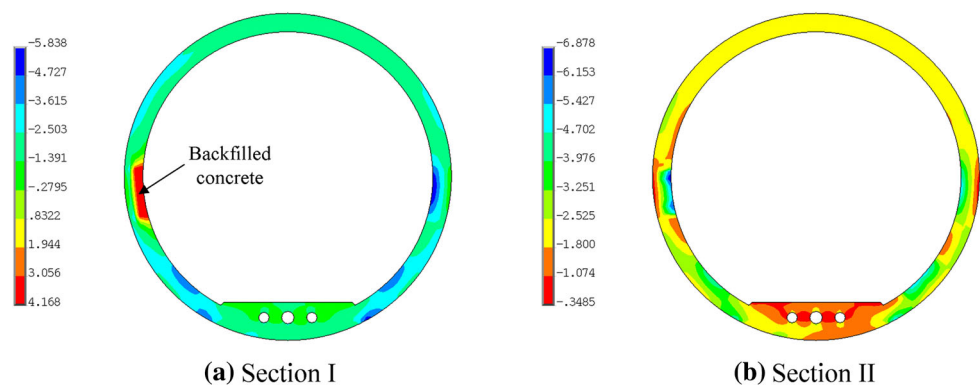
(b) Section II

experiment. The distribution of the observation points and the observation sections are shown in Figs. 3 and 4, respectively. The results of the full-scaled simulation experiment are presented in Table 3.

The tension condition is divided into two processes. The first process is that all the anchor cables are tensioned to 1000 kN and the second process is that all the anchor cables are tensioned to 2250 kN. Before the tension, some tensile stresses or compressive stresses appear on the intrados surface of the secondary lining because of the gravity, defect treatment and backfill grouting. However, these stresses are very small. After the first process of the tension condition, all the observation points are compressed obviously. When the second process is complete, the compressive stresses are further increased, and the stresses of the observation points range from −12.99 to −3.83 MPa.

The compressive stresses of almost all the observation points before water-filled condition are slightly larger than those after the second process of the tension condition because of the influence of duct grouting and groove backfilling. When the tunnel is under the water-filled condition, the compressive stresses of the observation points are decreased because of the internal water pressures, and the stresses of the observation points range from −7.91 to −1.33 MPa. All the observation points are still compressed.

As shown in Table 3, no matter which working condition it is, both the experimental results and the numerical results show that the compressive stresses of observation points below the springline are relatively large. Because the grooves are concentrated below the springline (Figs. 3, 4) and the effective prestresses of the anchor cables near the grooves are relatively large (Fig. 11).
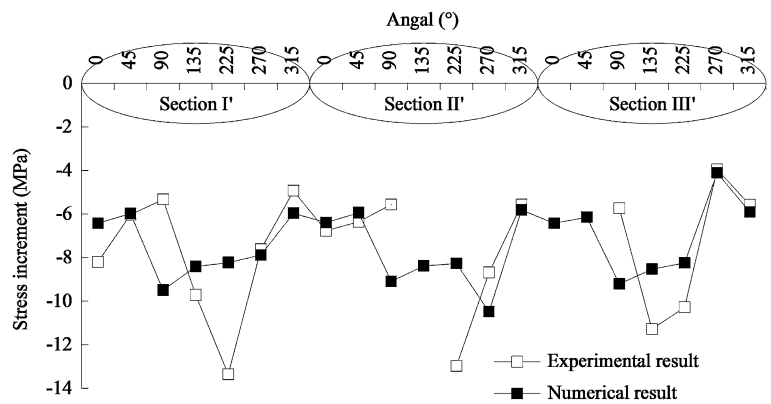
5.4.2 Circumferential Stresses Increment of the Secondary Lining

The circumferential compressive stress increments of the secondary lining caused by the prestresses are presented in Fig. 17. Large circumferential compressive stress increments of the secondary lining are caused by the prestresses, especially below the springline. The average stress increment of the observation points is −7.66 MPa in the full-scaled simulation experiment, and the average stress increment of the nodes correspond to the observation points is −7.46 MPa in the numerical calculation. The circumferential tensile stress increments of the secondary lining caused by the internal water pressures are presented in Fig. 18. The average stress increment of observation points is 3.94 MPa in the full-scaled simulation experiment, and the average stress increment of the nodes correspond to the observation points is 3.98 MPa in the numerical calculation.

Table 3 Results of the full-scaled simulation experiment (unit: MPa)

Section	Position (°)	Tension condition				Water-filled condition		
		Before tension	First process	Second process	Numerical results	Before water-filled	After water-filled	Numerical results
I–I	0	0.18	−5.32	−8.02	−6.28	−8.72	−2.23	−2.44
	45	−0.03	−4.12	−6.04	−6.20	−6.67	−3.36	−2.19
	90	−0.20	−3.70	−5.53	−9.69	−5.90	−3.50	−5.50
	135	1.24	−5.15	−8.47	−8.78	−9.55	−4.64	−4.98
	225	0.38	−7.95	−12.99	−8.50	−14.33	−7.91	−4.72
	270	−0.43	−5.37	−8.05	−8.06	−8.71	−5.73	−4.13
	315	−0.18	−3.43	−5.11	−6.16	−5.46	−1.99	−2.16
II–II	0	−0.49	−4.85	−7.25	−6.25	−7.55	−1.33	−2.41
	45	0.34	−3.98	−6.01	−6.16	−6.66	−3.78	−2.16
	90	0.36	−3.25	−5.20	−9.31	−5.42	−3.10	−5.10
	135	–	–	–	−8.75	–	–	−4.98
	225	1.84	−6.12	−11.12	−8.55	–	–	−4.78
	270	−0.13	−5.78	−8.81	−10.68	–	–	−6.48
	315	−0.19	−3.94	−5.75	−6.02	−6.63	−3.72	−2.03
III–III	0	–	–	–	−6.28	–	–	−2.44
	45	–	–	–	−6.35	–	–	−2.34
	90	0.33	−3.33	−5.39	−9.41	−5.52	−3.04	−5.22
	135	0.39	−6.68	−10.89	−8.82	−12.50	−7.16	−5.04
	225	0.57	−5.68	−9.70	−8.60	−10.54	−5.87	−4.82
	270	0.12	−2.49	−3.83	−4.11	−4.28	−1.69	−0.29
	315	−0.31	−4.06	−5.88	−6.12	−6.60	−3.27	−2.12

Fig. 17 Circumferential stress increments caused by the prestresses

Fig. 18 Circumferential stress increments caused by the internal water pressure
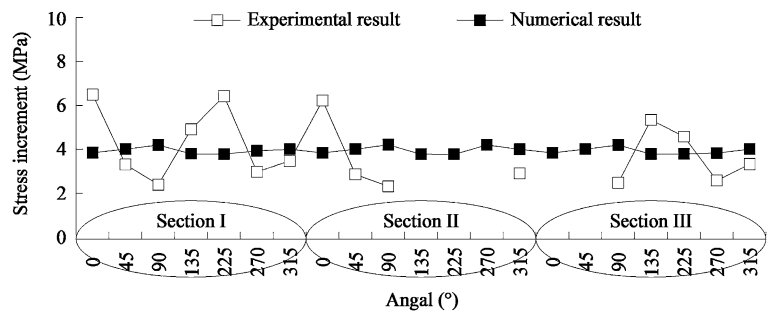
Several strain gauges are broken and the experimental results of several observations have some errors compared with the numerical calculation. That may be because the concrete vibrator or some other interference factors have affected the strain gauges during the construction of the experimental model. However, the calculated stresses of most of the observation points approximate to the experimental results (Table 3), and the stress increments of the numerical results are roughly consistent with the experimental results (Figs. 17, 18).

6 Conclusions

Based on the characteristics of the prestressed composite lining of the Yellow River Crossing Tunnel in MRP-SNWD, a three-dimensional solid model is established by finite element method. The performances of the segmental lining, the secondary lining and the stress transmission between the segmental lining and the secondary lining are studied. Some conclusions about the prestressed composite lining can be drawn.

Some prestresses and internal water pressures can be transmitted to the bottom of the segmental lining. But the segmental joints almost can not be further open and full circular compression can be realized for the secondary lining when the tunnel is under the water-filled condition. Besides, the membrane can play a role in waterproof and drainage. Therefore, the difficult problem for the Yellow River Crossing Tunnel that the internal water leaking out has been solved.

Because of the membrane, the interface gap above the springline of the lining is open when the tunnel is under the tension condition, and the interface gap decreases under the water-filled condition. So the stresses above the springline of the lining cannot be transmitted between the segmental lining and the secondary lining. The membrane below the springline of the lining is compressed, while the compression stresses are very small. Therefore, the membrane can play a significant role in preventing stress transmission.

Both the prestresses and the internal water pressure can cause obvious circumferential stress increments of the secondary lining. The stresses and stress increments calculated by the numerical model are in agreement with the experimental result, which verifies the feasibility of the numerical simulation.

The MRP-SNWD has been put into use. The numerical results in this paper and the actual operation of the project show that the prestressed composite lining used in the Yellow River Crossing Tunnel has an ideal performance in the shield tunnel for water conveyance and other similar projects with characteristics such as high internal pressure, poor geological conditions, high anti-seepage requirement, etc.

References

1. Kang JF, Hu YM (2005) Techniques and performance of post-prestressed tunnel liner. Pract Period Struct Des Constr 10(2):102–108
2. Grunicke UH, Ristić M (2012) Pre-stressed tunnel lining-pushing traditional concepts to new frontiers/Neue Grenzen für Passiv Vorgespannte Druckstollenauskleidungen. Geomech Tunn 5(5):503–516
3. Lee KM, Hou XY, Ge XW, Tang Y (2001) An analytical solution for a jointed shield-driven tunnel lining. Int J Numer Anal Meth Geomech 25(4):365–390
4. Ding WQ, Yue ZQ, Tham LG, Zhu HH, Lee CF, Hashimoto T (2004) Analysis of shield tunnel. Int J Numer Anal Meth Geomech 28(1):57–91
5. Do NA, Dias D, Oreste P, Djeran-Maigre I (2013) 2D numerical investigation of segmental tunnel lining behavior. Tunn Undergr Space Technol 37:115–127
6. Yang YZ, Zhang WW, Wang JW, Yang ZH (2014) Three-dimensional orthotropic equivalent modelling method of large-scale circular jointed lining. Tunn Undergr Space Technol 44:33–41
7. Blom CBM, Van der Horst EJ, Jovanovic PS (1999) Three-dimensional structural analyses of the shield-driven "Green Heart" tunnel of the high-speed line south. Tunn Undergr Space Technol 14(2):217–224
8. Li XK, Zhao SB, Zhao GF (2004) Theoretical analysis of pre-stressed concrete penstock under uni-ring-like prestress. J Dalian Univ Technol 44(2):277–283 **(in Chinese)**
9. Li XK, Zhao SB, Zhao GF (2004) Design Methods of Prestressed Concrete Penstock. Eng Mech 21(6):124–130 **(in Chinese)**
10. ITA (2000) Guidelines for the design of shield tunnel lining. Tunn Undergr Space Technol 15(3):303–331
11. Murakami H, Koizumi A (1987) Behavior of shield segment ring reinforced by secondary lining. J Jpn Soc Civ Eng 388:85–94 **(in Japanese)**
12. Takamatsu N, Murakami H, Koizumi A (1992) A Study on the Bending Behavior in the Longitudinal Direction of Shield Tunnels with Secondary Linings. In: Proceedings of the International Congress on 'Towards New World in Tunnellings', Acapulco, pp 227–285
13. Zhang HM, Guo C, Lu GL (2001) Mechanical model for shield pressure tunnel with secondary linings. J Hydraul Eng 4:28–33 **(in Chinese)**
14. Yan QX, Yao CF, Yang WB, He C, Geng P (2015) An Improved Numerical Model of Shield Tunnel with Double Lining and Its Applications. Adv Mater Sci Eng
15. Duan GX, Xu H (2011) Analysis on stress observation results of full-scaled lining simulation model of tunnel crossing Yellow River. Yangtze River 42(8):87–91 **(in Chinese)**
16. Chandrupatla TR, Belegundu AD, Ramesh T, Ray C (2002) Introduction to finite elements in engineering. Prentice Hall, Upper Saddle River
17. Kim J, Yoon JC, Kang BS (2007) Finite element analysis and modeling of structure with bolted joints. Appl Math Model 31(5):895–911

18. Mo HH, Chen JS (2008) Study on inner force and dislocation of segments caused by shield machine attitude. Tunn Undergr Space Technol 23(3):281–291

19. Chen JS, Mo HH (2009) Numerical study on crack problems in segments of shield tunnel using finite element method. Tunn Undergr Space Technol 24(1):91–102

20. Yousaf M, Siddiqi ZA, Sharif MB, Qazi AU (2016) Force and Displacement-controlled Non-linear FE Analyses of RC Beam with Partial Steel Bonded Length. Int J Civ Eng. doi:10.1007/s40999-016-0076-4

21. Mashimo H, Ishimura T (2003) Evaluation of the load on shield tunnel lining in gravel. Tunn Undergr Space Technol 18(2):233–241

22. GB 50010 (2010) Code for Design of Concrete Structure. China Architecture and Building Press, Beijing

23. Ma H, Zhang D (2016) Seismic Response of a Pre-stressed Concrete Wind Turbine Tower. Int J Civ Eng. doi:10.1007/s40999-016-0029-y